JACS
JOURNAL OF THE AMERICAN CHEMICAL SOCIETY

Communication

pubs.acs.org/JACS

Synthesis, Electronic Structure, and Magnetism of $[Ni(6\text{-}Mes)_2]^+$: A Two-Coordinate Nickel(I) Complex Stabilized by Bulky N-Heterocyclic Carbenes

Rebecca C. Poulten,[†] Michael J. Page,[†] Andrés G. Algarra,[‡] Jennifer J. Le Roy,[§] Isidoro López,[∥] Emma Carter,[⊥] Antoni Llobet,*[,∥] Stuart A. Macgregor,*[,‡] Mary F. Mahon,[†] Damien M. Murphy,[⊥] Muralee Murugesu,*[,§] and Michael K. Whittlesey*[,†]

[†]Department of Chemistry, University of Bath, Bath BA2 7AY, U.K.

[‡]Institute of Chemical Sciences, School of Engineering and Physical Sciences, Heriot-Watt University, Edinburgh EH14 4AS, U.K.

[§]Department of Chemistry, University of Ottawa, 10 Marie Curie, Ottawa, Ontario, Canada K1N 6N5

[∥]Institute of Chemical Research of Catalonia (ICIQ), Avinguda Paisos Catalans 16, E-43007 Tarragona, Spain

[⊥]School of Chemistry, Cardiff University, Main Building, Park Place, Cardiff CF10 3AT, U.K.

Supporting Information

ABSTRACT: The two-coordinate cationic Ni(I) bis-N-heterocyclic carbene complex $[Ni(6\text{-}Mes)_2]Br$ (**1**) [6-Mes =1,3-bis(2,4,6-trimethylphenyl)-3,4,5,6-tetrahydropyrimidin-2-ylidene] has been structurally characterized and displays a highly linear geometry with a C−Ni−C angle of 179.27(13)°. Density functional theory calculations revealed that the five occupied metal-based orbitals are split in an approximate 2:1:2 pattern. Significant magnetic anisotropy results from this orbital degeneracy, leading to single-ion magnet (SIM) behavior.

The strategy of employing sterically encumbered ligands for the stabilization of low-coordinate transition-metal complexes has proven to be particularly useful for the isolation of ML_2 species.[1] Bulky amide, alkyl, and aryl groups have all been utilized for the synthesis of stable first-row metal derivatives for V to Ni with open-shell electronic configurations. In a recent review, Power noted that among the structurally characterized examples, <20% display a strictly linear geometry.[2] Such species are of particular interest as they may display unquenched first-order orbital angular momentum, thus generating intrinsic magnetic anisotropy.[3] Molecules with a nonzero spin ground state and significant anisotropy can give rise to a barrier to the magnetization relaxation. Such molecules are termed single-molecule magnets (SMMs), and they have promising applicability in molecular electronics.[4] In recent years, mononuclear cobalt and iron complexes have shown single-ion magnet (SIM) behavior,[3c−f] but no other mononuclear SIMs based on transition metals have been reported. Here we report that the cationic, two-coordinate Ni(I) N-heterocyclic carbene (NHC) complex $[Ni(6\text{-}Mes)_2]Br$ (**1**)[5] exhibits SMM behavior as a result of orbital degeneracy. The presence of the two bulky six-membered-ring NHC ligands enforces a highly linear geometry in **1**, which represents only the second fully characterized example of a two-coordinate Ni(I) species.[6]

Complex **1** was isolated as a cream-colored solid in 60% yield upon addition of 1 equiv of the free six-membered NHC 6-Mes to a THF solution of the three-coordinate Ni(I) species Ni(6-Mes)(PPh_3)Br.[7] Despite having a formal electron count of 13, **1** could be handled in air for several minutes without any change in color; indeed, no change in the paramagnetic NMR spectrum was observed over 30 min even upon exposure of a CD_2Cl_2 solution of the complex to air! The X-ray crystal structure (Figure 1)[8] revealed a highly linear system [C−Ni−C angle of 179.27(13)°] with Ni−C distances of 1.939(3) and 1.941(3) Å. The Ni(I) ion is encapsulated in a cage formed by the mesityl groups, thus preventing any further coordination. No close contacts to the mesityl substituents were apparent from the X-ray data. In the crystal lattice, one Br^- counterion and two CH_2Cl_2 molecules of crystallization were found [Figures S1 and S2 in the Supporting Information (SI)]. Close

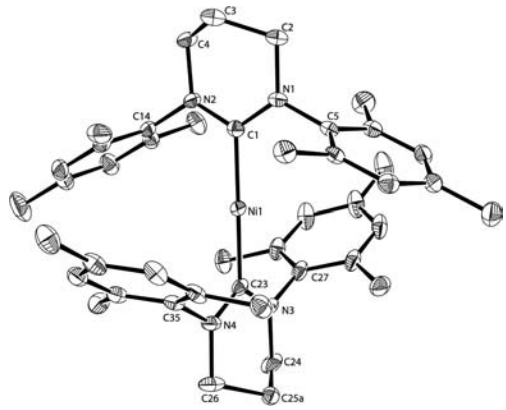

Figure 1. X-ray crystal structure of the cation in $[Ni(6\text{-}Mes)_2]Br$ (**1**). H atoms have been omitted for clarity. Thermal ellipsoids are shown at 30% probability.

Received: July 9, 2013
Published: August 23, 2013

dx.doi.org/10.1021/ja407004y | J. Am. Chem. Soc. 2013, 135, 13640−13643

inspection of the packing arrangement revealed a closest Ni···Ni distance of 10.3 Å, thus precluding any intermolecular magnetic interactions (vide infra).

A cyclic voltammogram of **1** (Figure 2) showed the presence of a chemically reversible ($i_{p,a}/i_{p,c}$ = 1.0) and electrochemically

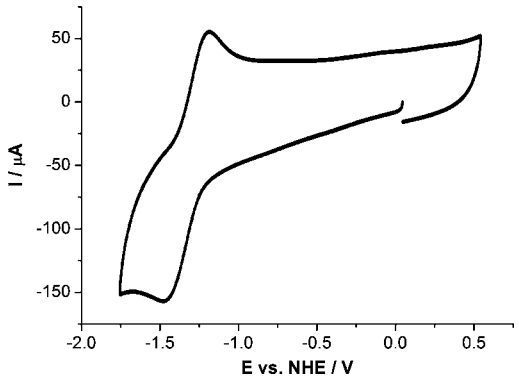

Figure 2. CV before electrolysis of a 0.5 mM solution of **1** in 0.1 M [*n*-Bu_4N]PF_6/THF. A carbon rod was used as the working electrode, a Pt wire as the counter electrode, and Ag/$AgNO_3$ (0.01 M in MeCN) as the reference electrode. Scan rate = 150 mV s^{-1}.

quasi-reversible ($E_{p,a} - E_{p,c}$ = 171 mV) wave associated with the one-electron reduction of Ni(I) to Ni(0) at −1.32 V vs NHE in THF. The one-electron nature of the process was corroborated by bulk electrolysis at an applied potential of −1.66 V (see the SI). Scanning anodically, a chemically irreversible wave was found at $E_{p,a}$ = 1.21 V that was assigned to the Ni(II)/Ni(I) couple (Figure S3). Chemical reduction of **1** was accomplished with KC_8 in THF to generate the Ni(0) derivative Ni(6-Mes)$_2$ (**2**), which was isolated as an extremely air-sensitive deep purple solid. A highly linear C−Ni−C geometry [177.71(10)°] is retained in the molecular structure of **2** (Figure 3)[9] but is accompanied by a distinct shortening of the Ni−C distances to 1.852(2) and 1.868(3) Å.

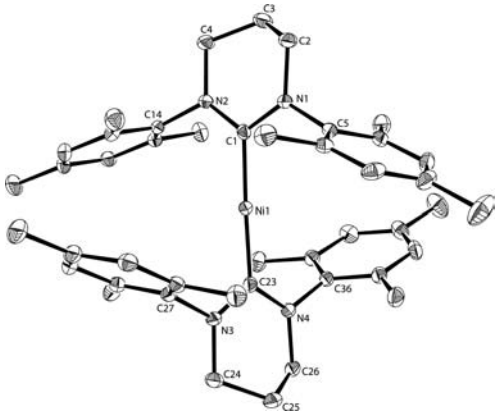

Figure 3. X-ray crystal structure of Ni(6-Mes)$_2$ (**2**). Hydrogen atoms are omitted for clarity. Thermal ellipsoids shown at 30% probability.

The key structural features of **1** and **2** were reproduced by density functional theory (DFT) calculations (BP86),[10] in particular the near-linear geometries of the two species and the shortening of the Ni−C distances upon reduction (average Ni−C_{calc}: 1.945 Å in **1**; 1.869 Å in **2**). The associated electronic structure is most clearly seen for the closed-shell species **2** (Figure 4), which exhibits five occupied metal-based orbitals in

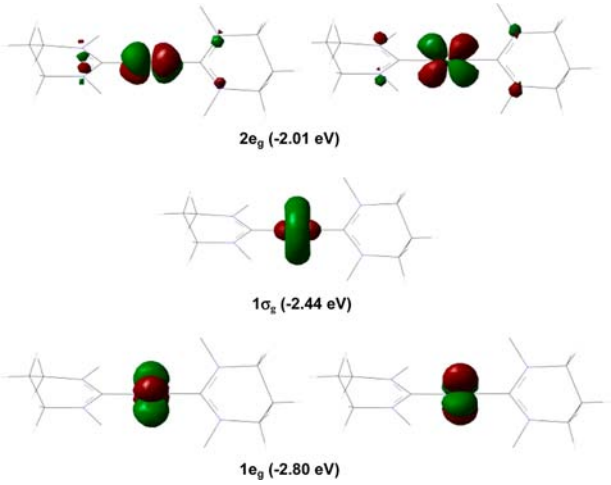

Figure 4. Highest-lying occupied molecular orbitals of **2**, with associated energies. Symmetry labels reflect local $D_{\infty h}$ symmetry at the metal center, and average energies are given for the e_g pairs (which differ in energy by <0.02 eV). Mesityl substituents have been truncated at the ipso carbon for clarity.

an approximate 2:1:2 splitting pattern. Within this, the near-degenerate HOMO corresponds to the Ni d_{xz} and d_{yz} orbitals, and these lie ca. 0.4 eV above a σ-type orbital at −2.44 eV that is dominated by Ni d_{z^2} and s character. The near-degenerate $d_{x^2-y^2}$ and d_{xy} orbitals are at −2.80 eV. A similar set of orbitals has been reported for Pd(NHC)$_2$ species, although in that case a 1:2:2 splitting of the orbitals was computed and confirmed by photoelectron spectroscopy.[11] For the current Ni system, removal of an electron from **2** to give **1** affords an orbitally degenerate system that is not readily described by a single-configuration DFT calculation (see Figure S4 for orbital plots and energies). The orbital degeneracy is central to understanding the magnetic properties of **1**.

Determination of the room-temperature magnetic moment in solution (Evans method) and the solid state (Gouy balance) gave μ_{eff} values of 2.2μ_B and 2.7μ_B, respectively. In contrast, X- and Q-band electron paramagnetic resonance (EPR) measurements undertaken on **1**, both as a solid powder and as a frozen solution at 4 K, showed no detectable EPR signals under any conditions. The absence of any detectable EPR signal may at least in part be attributed to the unquenched orbital angular momentum experienced in **1** (vide infra), which should lead to large *g* shifts,[12] and the significant orbital degeneracy predicted by DFT.

To further elucidate the magnetic properties, solid-state superconducting quantum interference device (SQUID) measurements were performed on crushed polycrystalline samples of **1**. The direct current (dc) magnetic properties were investigated under a 1000 Oe dc field over the temperature range 1.8−300 K (Figure S5). The room-temperature χT value of 1.12 cm^3 K mol^{-1} is much higher than the expected theoretical spin-only value of 0.375 cm^3 K mol^{-1} for a d^9 Ni(I) complex [$S = {}^1/_2$, $g = 2$, $\chi T = g^2S(S+1)/8$]. This value is also consistent with the observed room-temperature value obtained by the Evans or Gouy balance method (vide supra). The abnormally high value can originate from significant inherent anisotropy of the Ni(I) ion due to its d-orbital splitting, which is related to that for **2** shown in Figure 4. The higher-energy d_{xz} and d_{yz} orbitals are close in energy and, being partially-filled, can interconvert by rotation of 90°

dx.doi.org/10.1021/ja407004y | J. Am. Chem. Soc. 2013, 135, 13640−13643

about the z axis. Hence, in the ground state, the orbital angular momentum is not quenched by the ligand field, leading to first-order orbital angular momentum and a sizable magnetic anisotropy, $|D|$.[3a,b] When we take into consideration the orbital contribution, the observed χT value of 1.12 cm^3 K mol^{-1} is in better agreement with the expected value of 1.57 cm^3 K mol^{-1} for a Ni(I) ion [$^2D_{5/2}$, $S = {}^1/_2$, $L = 2$, $J = {}^5/_2$, $g = {}^6/_5$, $\chi T = g^2J(J + 1)/8$] with unquenched orbital angular momentum. As the temperature was decreased, the χT product remained nearly constant until a slight decrease below 10 K, reaching a minimum value of 1.00 cm^3 K mol^{-1}. Such behavior is consistent with a noninteracting mononuclear complex.

To further confirm the presence of magnetic anisotropy, field-dependent magnetization measurements were carried out between 1.8 and 7 K at fields ranging from 0 to 7 T (Figure S6). The magnetization data below 7 K revealed a rapid increase in the magnetization at low magnetic fields. Above 2 T a more gradual increase was observed, reaching near-saturation at low temperatures ($M = 2.45\mu_B$ at 1.8 K under 7 T). The nonsaturation as well as the non-superimposition of isotemperature lines in the M vs H/T plot again suggest magnetic anisotropy in **1** (Figure S6).

To probe the magnetic relaxation dynamics of **1**, alternating current (ac) magnetic susceptibility measurements were performed. Under zero applied dc field, no out-of-phase (χ'') signal was observed. Under a 600 Oe applied dc field, **1** displayed a strong temperature- and frequency-dependent χ'' signal (Figures 5 and S7). Temperature-dependent χ'' data revealed full frequency-dependent peaks with peak maxima shifting toward lower temperatures (Figure S6). Such slow relaxation of the magnetization is consistent with field-induced SMM behavior. Similarly, the frequency-dependent data revealed increasing χ'' with decreasing temperature and frequency over the temperature range 9−1.8 K, further indicating SIM behavior. The frequency-dependent data and the Arrhenius equation [$\tau = \tau_0 \exp(U_{eff}/kT)$] were used to extract the anisotropic barrier, $U_{eff} = 17$ K, and the τ_0 value of 4.6×10^{-6} s (Figure S8). Although relatively small, the energy barrier signifies that **1** is the first mononuclear Ni complex to display SIM behavior.

The energy barrier against spin reversal was surprisingly only observed under an applied dc field. Such a bias is necessary to suppress quantum tunneling of the magnetization (QTM), which leads to fast relaxation dynamics. QTM is minimized in Kramers ions, which should not require an applied field to demonstrate slow relaxation dynamics.[3a,b,g] Complex **1** has a half-integer spin, and SQUID analysis confirmed significant anisotropy. Therefore, the absence of zero-field slow relaxation dynamics most likely results from mixing between the degenerate ground and thermally accessible excited electronic states. In recent years, several Ni complexes with very large anisotropy values have been reported;[13] however, no mononuclear complex exhibiting single-ion magnet behavior has been reported.

In summary, we have described the use of very bulky N-heterocyclic carbene ligands to prepare [Ni(6-Mes)$_2$]Br (**1**), a very rare example of a two-coordinate Ni(I) complex. The analogous closed-shell Ni(0) complex **2** was obtained through reduction of **1**. SQUID measurements on this tunable highly linear complex **1** revealed that it is the first mononuclear Ni complex to display single-ion magnet behavior. This arises as a direct result of the 2:1:2 splitting of the occupied metal-based orbitals determined computationally. Efforts to prepare analogues of **1** are in progress.

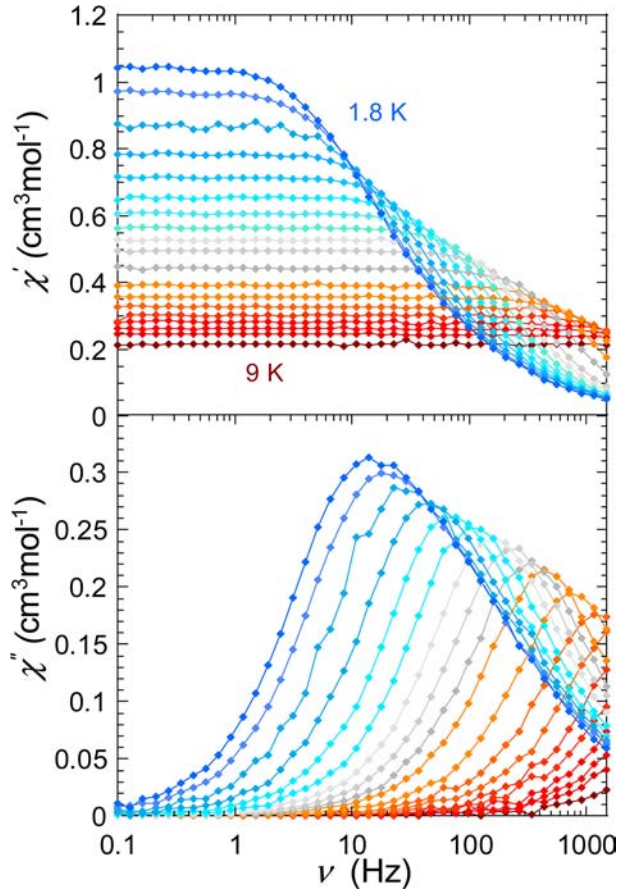

Figure 5. Frequency dependence of the in-phase (top) and out-of-phase (bottom) susceptibility between 1.8 and 9 K under a 600 Oe applied dc field.

■ ASSOCIATED CONTENT

Ⓢ Supporting Information

Experimental procedures and analysis for **1** and **2**, crystallographic data (CIF), bulk electrochemical and SQUID magnetic data on **1**, computed Cartesian coordinates and energies, orbital plots, and complete ref 10 (as SI ref 5). This material is available free of charge via the Internet at http://pubs.acs.org.

■ AUTHOR INFORMATION

Corresponding Author

m.k.whittlesey@bath.ac.uk

Notes

The authors declare no competing financial interest.

■ ACKNOWLEDGMENTS

We are grateful to the University of Bath, EPSRC, NSERC, and CFI for funding and Professor Dominic Wright (University of Cambridge) for experimental assistance. A.L. acknowledges support from MINECO (CTQ2010−21497) and A.G.A. thanks the Spanish Government for a Postdoctoral Fellowship (EX2009-0398).

■ REFERENCES

(1) (a) Buttrus, N. H.; Eaborn, C.; Hitchcock, P. B.; Smith, J. D.; Sullivan, A. C. *J. Chem. Soc., Chem. Commun.* **1985**, 1380. (b) Bartlett,

R. A.; Power, P. P. *J. Am. Chem. Soc.* **1987**, *109*, 7563. (c) Chen, H.; Bartlett, R. A.; Dias, H. V. R.; Olmstead, M. M.; Power, P. P. *J. Am. Chem. Soc.* **1989**, *111*, 4338. (d) Power, P. P. *J. Organomet. Chem.* **2004**, *689*, 3904. (e) Wolf, R.; Brynda, M.; Ni, C.; Long, G. J.; Power, P. P. *J. Am. Chem. Soc.* **2007**, *129*, 6076. (f) Kays, D. L. *Dalton Trans.* **2011**, *40*, 769.

(2) Power, P. P. *Chem. Rev.* **2012**, *112*, 3482.

(3) (a) Kahn, O. *Molecular Magnetism*; Wiley-VCH: New York, 1993. (b) Gatteschi, D.; Sessoli, R.; Villain, J. *Molecular Nanomagnets*; Oxford University Press: New York, 2006. (c) Zadrozny, J. M.; Xiao, D. J.; Atanasov, M.; Long, G. J.; Grandjean, F.; Neese, F.; Long, J. R. *Nat. Chem.* **2013**, *5*, 577. (d) Weismann, D.; Sun, Y.; Lan, Y.; Wolmershäuser, G.; Powell, A. K.; Sitzmann, H. *Chem.—Eur. J.* **2011**, *17*, 4700. (e) Lin, P.-H.; Smythe, N. C.; Gorelsky, S. I.; Maguire, S.; Henson, N. J.; Korobkov, I.; Scott, B. L.; Gordon, J. C.; Baker, R. T.; Murugesu, M. *J. Am. Chem. Soc.* **2011**, *133*, 15806. (f) Mossin, S.; Tran, B. L.; Adhikari, D.; Pink, M.; Heinemann, F. W.; Sutter, J.; Szilagyi, R. K.; Meyer, K.; Mindiola, D. J. *J. Am. Chem. Soc.* **2012**, *134*, 13651. (g) Bryan, A. M.; Merrill, W. A.; Reiff, W. M.; Fettinger, J. C.; Power, P. P. *Inorg. Chem.* **2012**, *51*, 3366.

(4) (a) Christou, G.; Gatteschi, D.; Hendrickson, D. N.; Sessoli, R. *MRS Bull.* **2000**, *25*, 66. (b) Thomas, L.; Lionti, L.; Ballou, R.; Gatteschi, D.; Sessoli, R.; Barbara, B. *Nature* **1996**, *383*, 145. (c) Freedman, D. E.; Jenkins, D.; Iavarone, A. T.; Long, J. R. *J. Am. Chem. Soc.* **2008**, *130*, 2884. (d) Maheswaran, S.; Chastanet, G.; Teat, S. J.; Mallah, T.; Sessoli, R.; Wernsdorfer, W.; Winpenny, R. E. P. *Angew. Chem., Int. Ed.* **2005**, *44*, 5044. (e) Milios, C. J.; Vinslava, A.; Wernsdorfer, W.; Prescimone, A.; Wood, P. A.; Parsons, S.; Perlepes, S. P.; Christou, G.; Brechin, E. K. *J. Am. Chem. Soc.* **2007**, *129*, 6547.

(5) 6-Mes = 1,3-bis(2,4,6-trimethylphenyl)-3,4,5,6-tetrahydropyrimidin-2-ylidene

(6) Laskowski, C. A.; Hillhouse, G. L. *J. Am. Chem. Soc.* **2008**, *130*, 13846.

(7) Page, M. J.; Lu, W. Y.; Poulten, R. C.; Carter, E.; Algarra, A. G.; Kariuki, B. M.; Macgregor, S. A.; Mahon, M. F.; Cavell, K. J.; Murphy, D. M.; Whittlesey, M. K. *Chem.—Eur. J.* **2013**, *19*, 2158.

(8) Crystal data for $[Ni(6\text{-Mes})_2]Br{\cdot}2CH_2Cl_2$ (**1**·$2CH_2Cl_2$) (CCDC 944018): $C_{46}H_{60}N_4Cl_4BrNi$, M = 949.40, monoclinic, a = 10.3210(1) Å, b = 21.8360(3) Å, c = 10.4070(2) Å, β = 94.612(1)°, V = 2337.82(6) Å^3, T = 150(2) K, space group $P2_1$, Z = 2, 46015 reflns measured, 10667 independent reflns (R_{int} = 0.0492). The final R_1 and $wR(F^2)$ values were 0.0365 and 0.0842, respectively [$I > 2\sigma(I)$]. Comparative values (all data) were 0.0567 and 0.0935.

(9) Crystal data for $[Ni(6\text{-Mes})_2]$ (**2**) (CCDC 944019): $C_{44}H_{56}N_4Ni$, M = 699.64, monoclinic, a = 10.3690(2) Å, b = 21.2180(5) Å, c = 17.6090(5) Å, β = 93.369(1)°, V = 3867.45(16) Å^3, T = 150(2) K, space group $P2_1/c$, Z = 4, 17846 reflns measured, 6348 independent reflns (R_{int} = 0.0518). The final $R1$ and $wR(F^2)$ values were 0.0436 and 0.0967, respectively [$I > 2\sigma(I)$]. Comparative values (all data) were 0.0620 and 0.1053.

(10) DFT calculations were run with the BP86 functional as implemented in Gaussian 03: Frisch, M. J., et al. *Gaussian 03*, revision D.01; Gaussian, Inc.: Wallingford, CT, 2004.

(11) (a) Green, J. C.; Scurr, R. G.; Arnold, P. L.; Cloke, F. G. N. *Chem. Commun.* **1997**, 1963. (b) Green, J. C.; Herbert, B. J. *Dalton Trans.* **2005**, 1214.

(12) (a) Rieger, P. H. *Electron Paramagnetic Resonance: Analysis and Interpretation*; RSC Publishing: Cambridge, U.K., 2007. (b) Weil, J. A.; Bolton, J. R.; Wertz, J. E. *Electron Paramagnetic Resonance: Elementary Theory and Practical Applications*; Wiley: New York, 1994.

(13) (a) Ruamps, R.; Maurice, R.; Batchelor, L.; Boggio-Pasqua, M.; Guillot, R.; Barra, A. L.; Liu, J.; Bendeif, E.-E.; Pillet, S. B.; Hill, S.; Mallah, T.; Guihery, N. *J. Am. Chem. Soc.* **2013**, *135*, 3017. (b) Krzystek, J.; Park, J.-H.; Meisel, M. W.; Hitchman, M. A.; Stratemeier, H.; Brunel, L.-C.; Telser, J. *Inorg. Chem.* **2002**, *41*, 4478. (c) Rogez, G.; Rebilly, J.-N.; Barra, A.-L.; Sorace, L.; Blondin, G.; Kirchner, N.; Duran, M.; van Slageren, J.; Parsons, S.; Ricard, L.; Marvilliers, A.; Mallah, T. *Angew. Chem., Int. Ed.* **2005**, *44*, 1876. (d) Ruamps, R.; Batchelor, L. J.; Maurice, R.; Gogoi, N.; Jiménez-Lozano, P.; Guihéry, N.; de Graaf, C.; Barra, A.-L.; Sutter, J.-P.; Mallah, T. *Chem.—Eur. J.* **2013**, *19*, 950.